phys. stat. sol. (b) **236**, No. 2, 318–324 (2003) / **DOI** 10.1002/pssb.200301671

Ab initio theory of exchange interactions in itinerant magnets

I. Turek[*,1,2], **J. Kudrnovský**[3,4], **V. Drchal**[3], **P. Bruno**[4], and **S. Blügel**[5]

[1] Institute of Physics of Materials, Academy of Sciences of the Czech Republic, Žižkova 22, 61662 Brno, Czech Republic
[2] Department of Electronic Structures, Charles University in Prague, Ke Karlovu 5, 12116 Prague 2, Czech Republic
[3] Institute of Physics, Academy of Sciences of the Czech Republic, Na Slovance 2, 18221 Prague 8, Czech Republic
[4] Max-Planck-Institut für Mikrostrukturphysik, Weinberg 2, 06120 Halle, Germany
[5] Institut für Festkörperforschung, Forschungszentrum Jülich, 52425 Jülich, Germany

Received 1 July 2002, accepted 15 October 2002
Published online 7 March 2003

PACS 75.10.Hk; 75.30.Et

The paper reviews an ab initio two-step procedure to determine thermodynamic properties of itinerant magnets. In the first step, the selfconsistent electronic structure of a system is calculated using the tight-binding linear muffin-tin orbital method combined with Green function techniques. In the second step, the parameters of the effective classical Heisenberg Hamiltonian are determined using the magnetic force theorem and they are employed in subsequent evaluation of magnon spectra, the spin-wave stiffness constants and the Curie/Néel temperatures. Applicability of the developed scheme is illustrated by investigations of selected properties of 3*d* metals Fe, Co, and Ni, diluted magnetic semiconductors (Ga,Mn)As, and 4*f* metals Gd and Eu.

1. Introduction Practical implementation of density-functional formalism led to excellent parameter-free description of ground-state properties of metallic magnets, including traditional bulk metals and ordered alloys as well as systems without the perfect three-dimensional periodicity (disordered alloys, surfaces, thin films). On the other hand, an accurate quantitative treatment of excited states and finite-temperature properties of these systems remains a challenge for *ab initio* theory of solids. The complexity of the problem calls for additional assumptions and approximations the validity of which has to be checked in each particular case. The purpose of this article is to review a recently developed first-principles scheme of this kind [1–3]. A brief presentation of the formalism and of the underlying physical ideas is accompanied by examples of applications to various bulk systems including transition metals, diluted magnetic semiconductors, and rare-earth metals. Applications to thin magnetic films can be found elsewhere [2, 4].

2. Formalism and numerical implementation The developed approach is based on a few simple physical assumptions: (i) the appropriate magnetic degrees of freedom of an itinerant magnetic system can be identified with atomic-like local magnetic moments created by correlated motion of electrons in the solid, (ii) these local moments can be treated as classical variables, and (iii) the corresponding

[*] Corresponding author: e-mail: turek@ipm.cz, Phone: +420 5 32290 437, Fax: +420 5 4121 8657

 0370-1972/03/23603-0318 $ 17.50+.50/0

energetics and dynamics can be described by an effective Heisenberg Hamiltonian (EHH)

$$H_{\mathrm{eff}} = -\sum_{\boldsymbol{R}\boldsymbol{R}'} J_{\boldsymbol{R}\boldsymbol{R}'}\, \boldsymbol{e}_{\boldsymbol{R}} \cdot \boldsymbol{e}_{\boldsymbol{R}'} \,. \tag{1}$$

In Eq. (1), the subscript $\boldsymbol{R}$ labels the lattice sites, the vectors $\boldsymbol{e}_{\boldsymbol{R}}$ are unit vectors pointing in the direction of the individual local moments, and the constants $J_{\boldsymbol{R}\boldsymbol{R}'}$ are parameters of the EHH which satisfy $J_{\boldsymbol{R}\boldsymbol{R}'} = J_{\boldsymbol{R}'\boldsymbol{R}}$ and $J_{\boldsymbol{R}\boldsymbol{R}} = 0$. The relevance of the local moments in an itinerant magnet can be justified by an adiabatic approximation [5], while the particular form of the Hamiltonian, Eq. (1), follows from a neglect of longitudinal fluctuations of the local magnetization as well as from results obtained for local moments at two impurity atoms in a non-magnetic host metal (for large impurity–impurity separations) [6] and for small deviations of the moment directions from a ferromagnetic ground state [7].

The zero-temperature spin dynamics of the EHH, Eq. (1), is well known. For ferromagnetic crystals with one atom in the primitive cell, the energy $E(\boldsymbol{q})$ of a magnon is related to the lattice Fourier transform $J(\boldsymbol{q})$ of the exchange interactions $J_{\boldsymbol{R}\boldsymbol{R}'}$ by

$$E(\boldsymbol{q}) = \frac{4\mu_{\mathrm{B}}}{M}\,[J(\boldsymbol{0}) - J(\boldsymbol{q})]\,, \qquad J(\boldsymbol{q}) = \sum_{\boldsymbol{R}} J_{\boldsymbol{0}\boldsymbol{R}} \exp\,(\mathrm{i}\boldsymbol{q}\cdot\boldsymbol{R})\,, \tag{2}$$

where $\boldsymbol{q}$ denotes a vector in the Brillouin zone (BZ) of the lattice, μ_{B} is the Bohr magneton and M denotes the local moment magnitude. For cubic systems and for small $\boldsymbol{q}$-vectors, $E(\boldsymbol{q}) \approx D|\boldsymbol{q}|^2$ with the spin-wave stiffness constant equal to

$$D = \frac{2\mu_{\mathrm{B}}}{3M} \sum_{\boldsymbol{R}} |\boldsymbol{R}|^2 J_{\boldsymbol{0}\boldsymbol{R}} \,. \tag{3}$$

The Curie temperature for the EHH can be expressed only approximatively. The simplest estimate is based on a mean-field approximation (MFA) which leads to

$$k_{\mathrm{B}} T_{\mathrm{C}}^{\mathrm{MFA}} = \tfrac{2}{3}\, J_0\,, \qquad J_0 = \sum_{\boldsymbol{R}} J_{\boldsymbol{0}\boldsymbol{R}}\,, \tag{4}$$

where k_{B} is the Boltzmann constant, whereas an improved formula for the Curie temperature is provided by a random-phase approximation (RPA) [8], namely

$$\left(k_{\mathrm{B}} T_{\mathrm{C}}^{\mathrm{RPA}}\right)^{-1} = \frac{3}{2}\,\frac{1}{N} \sum_{\boldsymbol{q}} [J(\boldsymbol{0}) - J(\mathbf{q})]^{-1}\,, \tag{5}$$

where N denotes the number of $\boldsymbol{q}$-vectors used in the BZ-average. It can be shown that $T_{\mathrm{C}}^{\mathrm{RPA}}$ is always smaller than $T_{\mathrm{C}}^{\mathrm{MFA}}$.

A standard *ab initio* evaluation of the parameters $J_{\boldsymbol{R}\boldsymbol{R}'}$ relies on the local spin-density approximation (LSDA) to the electronic structure of a system with a collinear spin structure, on the magnetic force theorem [7], and on a technique using local orbitals. Within the tight-binding linear muffin-tin orbital (TB-LMTO) method and the atomic-sphere approximation (ASA) [9, 10], the exchange interactions can be expressed as [1, 3, 6, 7]

$$J_{\boldsymbol{R}\boldsymbol{R}'} = -\,\frac{1}{8\pi\mathrm{i}} \int_C \mathrm{tr}_L[\boldsymbol{\Delta}_{\boldsymbol{R}}(z)\, g^{\uparrow}_{\boldsymbol{R}\boldsymbol{R}'}(z)\, \boldsymbol{\Delta}_{\boldsymbol{R}'}(z)\, g^{\downarrow}_{\boldsymbol{R}'\boldsymbol{R}}(z)]\,\mathrm{d}z\,, \tag{6}$$

where tr_L denotes the trace over the angular momentum index $L = (\ell m)$ and energy integration is performed in the complex energy plane over a closed contour C starting and ending at the Fermi energy (with the occupied part of the valence band lying inside C). The quantities $g^{\sigma}_{\boldsymbol{R}\boldsymbol{R}'}(z)$ $(\sigma = \uparrow, \downarrow)$ denote site-off-diagonal blocks of the so-called auxiliary Green-function matrices with elements $g^{\sigma}_{\boldsymbol{R}L,\boldsymbol{R}'L'}(z)$ while $\Delta_{\boldsymbol{R}}(z) = P^{\uparrow}_{\boldsymbol{R}}(z) - P^{\downarrow}_{\boldsymbol{R}}(z)$ are diagonal matrices related to the potential functions $P^{\sigma}_{\boldsymbol{R}\ell}(z)$ of the TB-LMTO method.

The results reported here are based on self-consistent LSDA calculations using the all-electron non-relativistic (scalar-relativistic) TB-LMTO-ASA method [10]. The subsequent calculation of the ex-

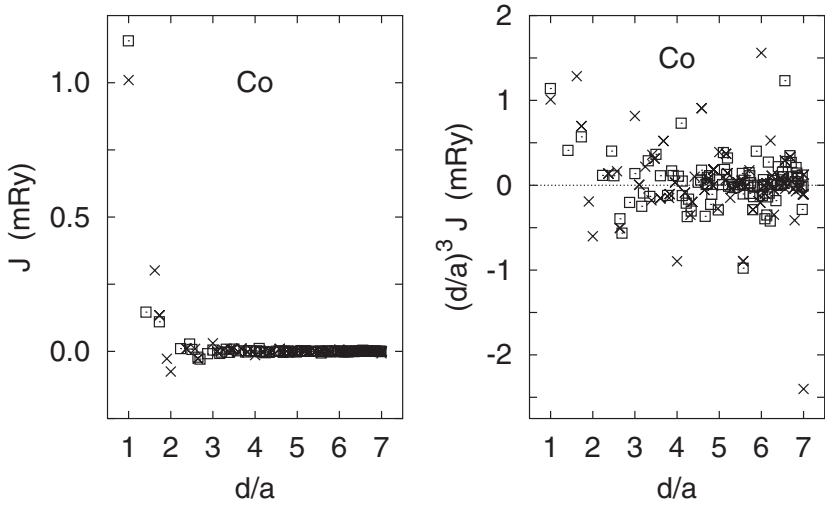

Fig. 1 Exchange interactions $J_{\boldsymbol{RR'}}$ for hcp Co as a function of the distance $|\boldsymbol{R}-\boldsymbol{R}'| = d$ without (left panel) and with (right panel) a prefactor d^3. The crosses and squares correspond to sites $\boldsymbol{R}$, $\boldsymbol{R}'$ lying in even and odd (0001) planes, respectively.

change interactions $J_{\boldsymbol{RR'}}$ for distances $d = |\boldsymbol{R}-\boldsymbol{R}'|$ up to ten lattice constants requires typically a few millions of $\boldsymbol{k}$-points in the full BZ-averages defining the site-off-diagonal blocks $g^{\sigma}_{\boldsymbol{RR'}}(z)$ in Eq. (6). More details can be found in Ref. [3].

3. Results

3.1 Transition metals The calculated Heisenberg exchange parameters for the hcp Co with experimental values of the lattice constants a and c are shown in Fig. 1. One can see the dominating ferromagnetic interactions for the first nearest-neighbor (1st-nn) shell followed by weaker interactions of both signs and decreasing magnitudes for bigger distances $d = |\boldsymbol{R}-\boldsymbol{R}'|$ (Fig. 1, left panel). The same qualitative features were found for the cubic $3d$ ferromagnets bcc Fe, fcc Co, and fcc Ni [3]. An analysis of Eq. (6) in the limit of large distances d reveals a Ruderman-Kittel-Kasuya-Yoshida (RKKY) asymptotic behavior [3]. This is illustrated in Fig. 1 (right panel) which proves undamped oscillations of the quantity $|\boldsymbol{R}-\boldsymbol{R}'|^3\, J_{\boldsymbol{RR'}}$.

The RKKY asymptotic behavior has pronounced influence of other quantities: in weak ferromagnets like bcc Fe it can give rise to Kohn anomalies in the magnon dispersion law, while in all cases it causes a rather slow convergence of the real-space sum in Eq. (2) and it leads even to a non-convergent sum for the spin-wave stiffness constant in Eq. (3). The latter fact requires a numerical procedure to obtain reliable values of D from the calculated exchange interactions [3]. The resulting values of the spin-wave stiffness constant and of the Curie temperatures for the three cubic ferromagnets are presented in Table 1 together with corresponding experimental values. One can see that satisfactory agreement for both D and T_{C} is obtained in the case of Fe and Co, in particular if the RPA value for T_{C} is taken for the comparison. On the other hand, big discrepancies are encountered for Ni, most

Table 1 Calculated spin-wave stiffness constants (D_{th}) and Curie temperatures ($T_{\mathrm{C}}^{\mathrm{MFA}}$ and $T_{\mathrm{C}}^{\mathrm{RPA}}$) and their comparison with experimental values D_{exp} and $T_{\mathrm{C,exp}}$

Metal	D_{th} [meV · Å^2]	D_{exp}[meV · Å^2]	$T_{\mathrm{C}}^{\mathrm{MFA}}$ [K]	$T_{\mathrm{C}}^{\mathrm{RPA}}$ [K]	$T_{\mathrm{C,exp}}$ [K]
Fe bcc	250 ± 7	280, 330	1414	950 ± 2	1044–1045
Co fcc	663 ± 6	580, 510	1645	1311 ± 4	1388–1398
Ni fcc	756 ± 29	555, 422	397	350 ± 2	624–631

probably due to the neglect of Stoner-like excitations in the EHH, Eq. (1), which are certainly of great importance for this system with a small exchange splitting.

3.2 Diluted magnetic semiconductors Diluted magnetic III–V semiconductors, represented by a compound $(Ga_{1-x}Mn_x)As$ with Mn-concentration in the range $0 < x < 0.1$, have recently attracted much interest because of the hole-mediated ferromagnetism [11, 12]. The Curie temperatures higher than the room temperature are desirable for practical applications, whereas the currently prepared samples exhibit the T_C around 100 K [12]. Since the Mn atoms are in the high-spin state in these systems, the above described formalism is well suited for reliable quantitative investigations of the exchange interactions and the Curie temperatures.

However, the (Ga,Mn)As compound is a substitutionally disordered system with Mn atoms substituting the Ga atoms on the cation sublattice, and the theory has to be modified accordingly. It can be shown that within the coherent-potential approximation (CPA) to the electronic structure of random alloys [10], the configurationally averaged exchange interaction between two particular atomic species, say two Mn atoms located at the lattice sites $\boldsymbol{R}$ and $\boldsymbol{R}'$, is given by a formula analogous to Eq. (6) with the Green-functions $g^{\sigma}_{\boldsymbol{R}\boldsymbol{R}'}(z)$ replaced by the so-called conditionally averaged Green-functions. The details of the self-consistent TB-LMTO-CPA method were given elsewhere [10], its application to the present system employs so-called empty spheres located at interstitial positions of GaAs semiconductor for matters of space filling.

The exchange interactions between the Mn atoms in the $(Ga_{1-x}Mn_x)As$ system with $x = 0.05$ are shown in Fig. 2 (left panel). The 1st-nn interaction is positive and bigger than the (mostly positive) interactions between more distant Mn atoms. The corresponding Curie temperature in the MFA is around 300 K, i.e., substantially higher than the experimental value. A possible source of this discrepancy can be found in structural imperfections of the compound which might lead to reduction of the number of holes in the valence band. Favorite candidates for such lattice defects are As-antisite atoms [11]. The combined effect of Mn-impurities and As-antisites can be simulated by an alloy $(Ga_{1-x-y}Mn_xAs_y)As$ with y denoting the As-antisite concentration. The dependence of the 1st-nn Mn–Mn interaction on x and y is shown in Fig. 2 (right panel) [13]. For a fixed Mn-concentration x, the 1st-nn exchange interaction decreaeses monotonously with increasing content of As-antisites y, ending finally at negative values. This change of sign nicely correlates with predicted instability of the ferromagnetic state with respect to formation of a state featured by disordered directions of the Mn-moments [13, 14].

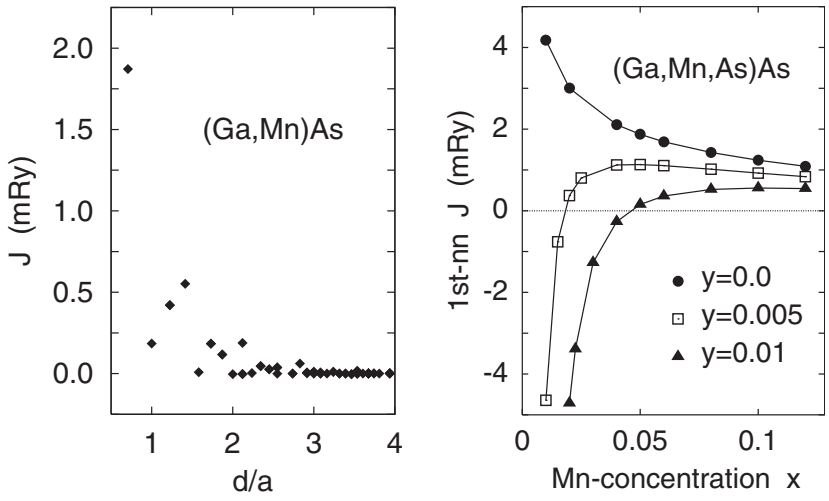

Fig. 2 The Mn–Mn exchange interactions in a $(Ga_{0.95}Mn_{0.05})As$ compound as a function of the Mn–Mn distance d (left panel) and the first nearest-neighbor Mn–Mn interaction in an alloy $(Ga_{1-x-y}Mn_xAs_y)As$ (right panel).

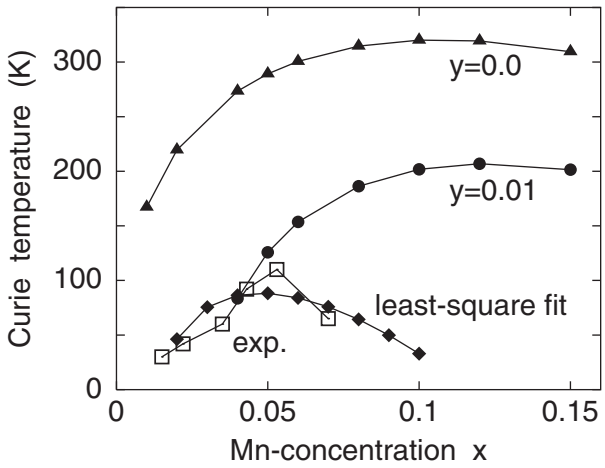

Fig. 3 Curie temperatures of $(Ga_{1-x-y}Mn_xAs_y)As$: calculated (full symbols) and experimental (open squares). For details, see text.

The resulting MFA-estimates of the Curie temperature are summarized in Fig. 3 [13]. The T_C for a fixed x is monotonously decreasing with increasing As-antisite concentration y, in analogy to the y-dependence of the 1st-nn Mn–Mn interaction. The T_C for a fixed y exhibits a non-monotonous dependence on the Mn-content x reaching a flat maximum for $x > 0.1$. The latter behavior results from an interplay of two effects [13]: (i) an increase of T_C with increasing x, which follows from Eq. (4) generalized to substitutionally disordered systems with non-negligible local moments carried only by one atomic species (Mn), and (ii) the non-trivial dependence of the 1st-nn Mn–Mn interaction as a function of (x, y), see Fig. 2 (right panel).

A detailed comparison of calculated and measured concentration dependences of the Curie temperature indicates a correlation between the two concentrations x and y in real samples, namely an increase of the As-antisite concentration with increasing Mn-content [13]. Assuming a linear relation $y = kx + y_0$ with unknown k and y_0, a least-square fit to the experimental Curie temperatures leads to reasonable semiquantitative reproduction of the measured values (Fig. 3). However, this agreement does not rule out alternative lattice defects in the system. Their influence on magnetic properties deserves further study.

3.3 Rare-earth metals The rare-earth metals represent another class of systems where the concept of atomic-like local moments is appropriate. The localized nature of $4f$ orbitals gives rise to large magnetic moments which however are coupled by s, p, and d electrons with much lower spin polarization. The ground-state properties of f-electron systems cannot be satisfactorily described using the LSDA. Here we treat the metals Gd (hcp structure) and Eu (bcc structure) in a simplified manner, namely with the $4f$ states taken as part of the core (with the majority $4f$ level occupied by 7 electrons and the minority $4f$ level empty). The rest of the valence orbitals are included in the standard LSDA. It has been shown recently that this approach yields reasonable results for the ground state of the hcp Gd [15].

The calculated total energies for the hcp Gd with an experimental value of $c/a = 1.597$ and for the bcc Eu as functions of the Wigner–Seitz radius s are shown in Fig. 4. Different spin configurations were considered: the ferromagnetic (FM), the antiferromagnetic (AFM) and the disordered local moment (DLM) state [5]. The theoretical equilibrium values of s ($s_{Gd} = 3.712$ a.u., $s_{Eu} = 4.190$ a.u.) are nearly insensitive to the spin structures and they are only slightly smaller than the experimental values ($s_{Gd} = 3.762$ a.u., $s_{Eu} = 4.263$ a.u.). The FM ground state of Gd exhibits a non-negligible energy separation from the AFM and DLM states in contrast to the bcc Eu, where the FM and DLM states are nearly degenerate.

The exchange interactions in Gd and Eu, derived for the FM state and the theoretical equilibrium Wigner–Seitz radius s, are shown in Fig. 5. Their distance-dependence is qualitatively similar to the hcp Co metal, the magnitudes of the dominating 1st-nn interactions are, however, smaller by a factor of five, cf. Fig. 1. Moreover, there is a profound difference between the two $4f$ metals concerning the

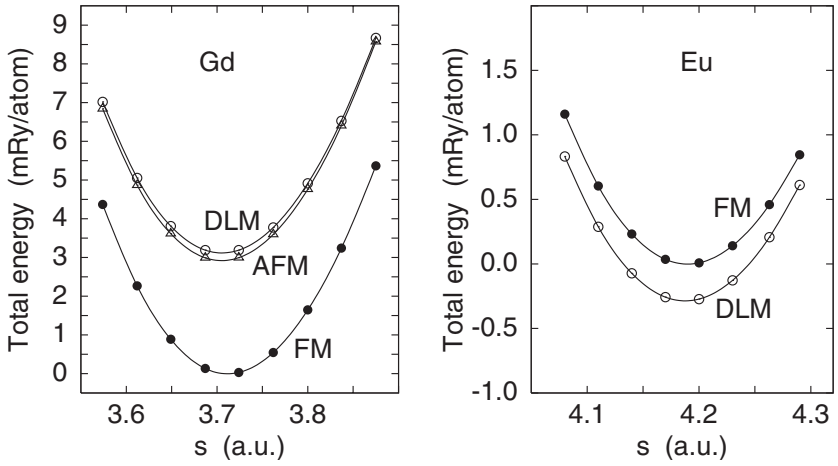

Fig. 4 Total energies for different magnetic states as functions of the Wigner-Seitz radius s for hcp Gd (left panel) and bcc Eu (right panel).

interactions of more distant atoms. In the hcp Gd, they are not strong enough to destroy the FM spin structure with the Curie temperature $T_C^{MFA} = 341\,K$, in good agreement with the measured value $T_{C,exp} = 293\,K$. In the case of bcc Eu, the contribution of more distant sites to the real-space sum in Eq. (4) is very important and it yields for the quantity $J_0 = J(\mathbf{0})$ a negligible resulting value ($J_0 = -0.03\,mRy$). Such a situation indicates an instability of the FM state with respect to a more complicated spin structure. This feature agrees qualitatively with an experimentally observed helical spin structure, the wave vector of which lies along the $\Gamma - H$ direction of the bcc BZ [16, 17].

A more quantitative specification of the non-collinear ground state of bcc Eu can be found on the basis of the lattice Fourier transform $J(\boldsymbol{q})$, Eq. (2). The minimum of the EHH, Eq. (1), occurs for a spin spiral with a wave vector $\boldsymbol{q} = \boldsymbol{Q}$ maximizing the $J(\boldsymbol{q})$. The calculated dependence of $J(\boldsymbol{q})$ along high-symmetry lines of the bcc BZ is shown in Fig. 6. A scan over the whole BZ reveals that the absolute maximum of $J(\boldsymbol{q})$ is obtained at a point inside the $\Gamma - H$ line, namely at $\boldsymbol{Q} = (1.685, 0, 0)\,a^{-1}$, where a denotes the bcc lattice constant. The magnitude of $\boldsymbol{Q}$ determines the angle ω between magnetic moments in the

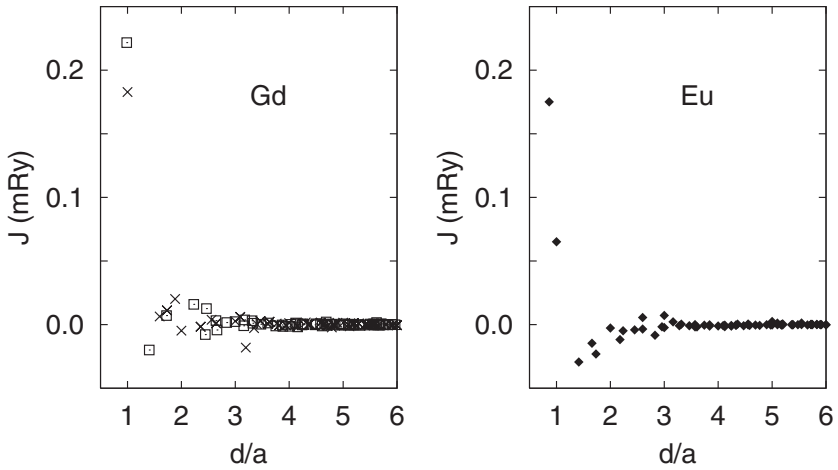

Fig. 5 Exchange interactions $J_{RR'}$ for hcp Gd (left panel) and bcc Eu (right panel) as functions of the distance $|\boldsymbol{R} - \boldsymbol{R}'| = d$. The crosses and squares in the left panel correspond to sites $\boldsymbol{R}$, $\boldsymbol{R}'$ lying in even and odd (0001) hcp planes, respectively.

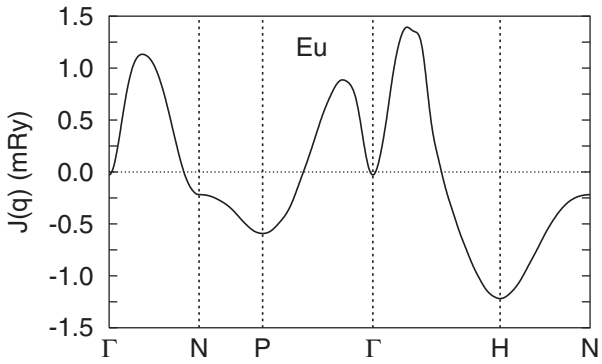

Fig. 6 The lattice Fourier transform $J(\boldsymbol{q})$ of the exchange interactions in bcc Eu along high-symmetry lines in the Brillouin zone.

neighboring (100) atomic planes. In the present case, it is equal to $\omega = 48^\circ$ in surprising agreement with measured values $\omega_{\mathrm{exp}} = 49^\circ$ [16] and $\omega_{\mathrm{exp}} = 47.6 \pm 1.2^\circ$ [17].

The resulting maximum $J(\boldsymbol{Q})$ can be used to get a MFA estimation of the Néel temperature, in complete analogy to Eq. (4). The value $T_{\mathrm{N}}^{\mathrm{MFA}} = 147\,\mathrm{K}$ is higher than the measured $T_{\mathrm{N,exp}} = 91\,\mathrm{K}$. The RPA estimations of the transition temperatures for both Gd and Eu are left for future studies – one can expect that the RPA will shift theoretical values closer to experiment.

4. Conclusions The most important feature of the described *ab initio* approach to exchange interactions lies in its real-space formulation, which makes it an efficient tool to handle: (i) long-range interactions encountered in itinerant magnets, and (ii) systems without three-dimensional translational invariance like, e.g., random alloys and low-dimensional magnets. The inherent limitation to cases with well-developed local magnetic moments does not seem to be a crucial disadvantage as a number of interesting systems with real or potential technological importance fall entirely within this class: magnetic transition-metal surfaces and ultrathin films, Mn-doped semiconductors, f-electron metals and compounds, etc.

Acknowledgements The authors acknowledge the support provided by the Grant Agency of the Czech Republic (No. 202/00/0122 and 106/02/0943), the Academy of Sciences of the Czech Republic (No. A1010203 and Z2041904), the Ministry of Education of the Czech Republic (COST P5.30 and MSM113200002), the Scientific and Technological Cooperation between Germany and the Czech Republic (No. TSR-013-98), and the RT Network 'Computational Magnetoelectronics' (Contract HPRN-CT-2000-00143) of the European Commission.

References

[1] V. P. Antropov, B. N. Harmon, and A. N. Smirnov, J. Magn. Magn. Mater. **200**, 148 (1999).
[2] M. Pajda, J. Kudrnovský, I. Turek, V. Drchal, and P. Bruno, Phys. Rev. Lett. **85**, 5424 (2000).
[3] M. Pajda, J. Kudrnovský, I. Turek, V. Drchal, and P. Bruno, Phys. Rev. B **64**, 174402 (2001).
[4] P. Bruno, J. Kudrnovský, M. Pajda, V. Drchal, and I. Turek, J. Magn. Magn. Mater. **240**, 346 (2002).
[5] B. L. Gyorffy, A. J. Pindor, J. Staunton, G. M. Stocks, and H. Winter, J. Phys. F **15**, 1337 (1985).
[6] A. Oswald, R. Zeller, P. J. Braspenning, and P. H. Dederichs, J. Phys. F **15**, 193 (1985).
[7] A. I. Liechtenstein, M. I. Katsnelson, V. P. Antropov, and V. A. Gubanov, J. Magn. Magn. Mater. **67**, 65 (1987).
[8] S. V. Tyablikov, Methods of Quantum Theory of Magnetism (Plenum Press, New York, 1967).
[9] O. K. Andersen and O. Jepsen, Phys. Rev. Lett. **53**, 2571 (1984).
[10] I. Turek, V. Drchal, J. Kudrnovský, M. Šob, and P. Weinberger, Electronic Structure of Disordered Alloys, Surfaces and Interfaces (Kluwer, Boston, 1997).
[11] H. Akai, Phys. Rev. Lett. **81**, 3002 (1998).
[12] H. Ohno, J. Magn. Magn. Mater. **200**, 110 (1999).
[13] J. Kudrnovský, I. Turek, V. Drchal, F. Máca, J. Mašek, and P. Weinberger, to be published.
[14] P. A. Korzhavyi et al., Phys. Rev. Lett. **88**, 187202 (2002).
[15] Ph. Kurz, G. Bihlmayer, and S. Blügel, J. Phys.: Condens. Matter **14**, 6353 (2002).
[16] N. G. Nereson, C. E. Olsen, and G. P. Arnold, Phys. Rev. **135**, A176 (1964).
[17] A. H. Millhouse and K. A. McEwen, Solid State Commun. **13**, 339 (1973).